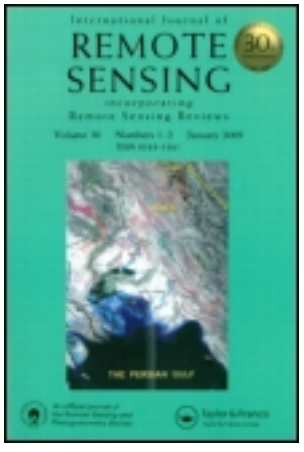

International Journal of Remote Sensing

Publication details, including instructions for authors and subscription information:
http://www.tandfonline.com/loi/tres20

Automated segmentation of vegetation structure units in a Mediterranean landscape

Avi Bar Massada [a], Rafi Kent [a], Lior Blank [a], Avi Perevolotsky [b], Liat Hadar [c] & Yohay Carmel [a]

[a] Faculty of Civil and Environmental Engineering, Technion - Israel Institute of Technology, Haifa, 32000, Israel

[b] Department of Agronomy and Natural Resources, Agricultural Research Organization, the Volcani Center, Bet Dagan, 50250, Israel

[c] Ramat Hanadiv Nature Park, Zichron Yaacov, 30900, Israel

Available online: 27 Oct 2011

To cite this article: Avi Bar Massada, Rafi Kent, Lior Blank, Avi Perevolotsky, Liat Hadar & Yohay Carmel (2012): Automated segmentation of vegetation structure units in a Mediterranean landscape, International Journal of Remote Sensing, 33:2, 346-364

To link to this article: http://dx.doi.org/10.1080/01431161.2010.532173

International Journal of Remote Sensing
Vol. 33, No. 2, 20 January 2012, 346–364

Taylor & Francis
Taylor & Francis Group

Automated segmentation of vegetation structure units in a Mediterranean landscape

AVI BAR MASSADA*†**, RAFI KENT†, LIOR BLANK†,
AVI PEREVOLOTSKY‡, LIAT HADAR§ and YOHAY CARMEL†
†Faculty of Civil and Environmental Engineering, Technion – Israel Institute of Technology, Haifa 32000, Israel
‡Department of Agronomy and Natural Resources, Agricultural Research Organization, the Volcani Center, Bet Dagan 50250, Israel
§Ramat Hanadiv Nature Park, Zichron Yaacov 30900, Israel

(*Received 13 October 2009; in final form 30 August 2010*)

In Mediterranean regions, the combination of disturbances, life histories, plant regeneration traits, and microhabitat variability form highly heterogeneous vegetation mosaics which shift in space and time. Consequently, structure-based forest management is emerging as a superior alternative to management of vegetation formations in such areas. Delineation of management units in these areas is often based on manual interpretation of aerial imagery coupled with field surveys. Here, we propose an alternative approach that is based on segmentation of remotely sensed height and cover maps derived from light detection and ranging (LiDAR) imagery. A large suite of alternative segmentation maps was generated using multiresolution segmentation (MS) with different parameters, and an area-fit approach used to select the map that most successfully captured a reference set of structural units delineated manually. We assessed the feasibility of this approach in a nature reserve in northern Israel, compared the resulting map with a traditional vegetation formations map, and explored the performance of the segmentation algorithm under various parameter combinations. Pronounced differences between the structure and formation maps highlight the suitability of this approach as an alternative to the existing methods of delineating vegetation units in Mediterranean systems, and possibly in other systems as well.

1. Introduction

Mediterranean landscapes have been affected by human disturbances for the past 10 000 years at least, resulting in the formation of structurally rich and diverse vegetation communities (Naveh and Dan 1973, Le Houerou 1981, Naveh and Kutiel 1986). As a result, these landscapes are often highly heterogeneous at a broad range of spatial scales, starting from a grain size as small as a few metres (Naveh 1975, Di Castri 1981, Noy-Meir *et al*. 1989, Pausas 1999, Shoshany 2000, Bar Massada *et al*. 2008).

*Corresponding author. Email: barmassada@wisc.edu
**Present address: Department of Forest and Wildlife Ecology, University of Wisconsin, Madison, WI, USA

International Journal of Remote Sensing
ISSN 0143-1161 print/ISSN 1366-5901 online © 2012 Taylor & Francis
http://www.tandf.co.uk/journals
http://dx.doi.org/10.1080/01431161.2010.532173

Mediterranean vegetation is also characterized by high structural variability, which is a product of spatio-temporal variation in the impact of disturbances, coupled with plant functional responses to these disturbances (Lavorel 1999). For planning and management of these complex landscapes, a structure-based vegetation classification may be more useful than the traditional botanically based vegetation maps, which often use terminologies that vary between regions and ignore temporal changes that may be ecologically significant.

Height and cover are the most basic and straightforward descriptors of vegetation structure (Tomaselli 1981, Kuchler 1988). Tomaselli (1981) developed a now widely used structural-physiognomic classification of Mediterranean shrubland vegetation (matorral) that is based on three components: height, cover and the morphology (e.g. thorny, deciduous or evergreen) of the predominant species. Other structure-based classifications of Mediterranean vegetation have been developed as well (Naveh and Whittaker 1979, Dufour Dror 2002).

While mapping cover has been a common practice since the earliest aerial photography, mapping height in detail and over large areas was less common until recent years owing to technical and methodological limitations. Mapping vegetation height has been greatly improved recently by active remote sensing instruments such as light detection and ranging (LiDAR) (e.g. Hinsley *et al*. 2002, Goodwin *et al*. 2006, Straatsma and Middelkoop 2006, Bergen *et al*. 2007). The use of LiDAR may be particularly valuable in Mediterranean vegetation, owing to its potential to yield very fine resolution products.

Mapping land and vegetation cover is usually carried out by image classification, which in most cases is pixel-based (De Jong *et al*. 2001). Pixel-based classification has been performed for a large variety of scales, techniques and purposes, and with different sensors. However, pixel-based classifiers generate textured results that are not readily usable for mapping management units. In heterogeneous landscapes, there is a large variability of reflectance values (even for similar entities such as vegetation types), which often yields fragmentary results. This may reduce the quality of land cover mapping (De Jong *et al*. 2001) and results may be useless for management (Lobo 1997).

The alternative approach, object-based classification, begins with image segmentation, followed by classification of image objects rather than pixels. This approach is better suited for identifying image entities that can later be used as vegetation structural units, since it allows for a certain level of spectral heterogeneity within each unit (Lamonaca *et al*. 2008). However, object-based classification is not free from disadvantages either, mainly the need to specify parameter values for the segmentation, where there is currently no understanding of the relations between these parameters and the structure and accuracy of the resulting segmented images (Hay *et al*. 2005).

There are many types of segmentation techniques, used in many scientific fields (e.g. quadtree segmentation (Samet 1990), iterative mutually optimum region merging (Lobo 1997), region-growing segmentation techniques (Lucieer and Stein 2005)).

One of the widely used segmentation methods is multiresolution segmentation (MS) (Baatz and Schäpe 2000, Benz *et al*. 2004). It operates at different scales, and uses a heuristic optimization procedure that locally minimizes the average heterogeneity of newly defined image objects for a given resolution, starting with individual pixels that are subsequently aggregated into objects. MS was applied to a QuickBird image of a beech forest in central Italy to delineate features of structural complexity, and a field survey was conducted to assess the differences between segmented

units (Lamonaca *et al*. 2008). The same method was used by Radoux and Defourny (2007) to automatically delineate forest stands in Belgium, in a study that assessed the accuracy of boundaries generated by the segmentation process. Object-based classification of QuickBird imagery based on both spectral and textural data was used to map structural classes of riparian and forest communities in British Columbia, Canada (Johansen *et al.* 2007). Chubey *et al.* (2006) applied an object-based classification of IKONOS-2 imagery to identify homogeneous landscape components in a mature forest ecosystem in Alberta, Canada. At a finer scale of analysis, Bunting and Lucas (2006) developed an iterative segmentation algorithm based on MS to delineate tree crowns from a high resolution Compact Airborne Spectrographic Imager (CASI) image, which was then combined with LiDAR data to assess forest biomass (Lucas *et al.* 2008).

One drawback of MS is that the user has to set a scale parameter that has an effect on the size of the resulting segments. Since this scale parameter has no relation to the size of actual image objects, it is necessary to evaluate alternative parameter values until an acceptable segmentation result is obtained. Hay *et al*. (2005) attempted to solve this problem by developing multiscale object-specific segmentation (MOSS), which yielded segmentation results at multiple scales. The method was tested on an IKONOS-2 panchromatic scene of southern Vancouver Island, Canada, where it was capable of automatically delineating objects at varying scales, from individual trees to forest stands. They concluded that the method could be particularly useful in future vegetation mapping for management purposes (Hay *et al*. 2005). Wang *et al*. (2004), mapping mangroves from IKONOS imagery on the Caribbean coast of Panama, developed a different approach for overcoming the problem of scale-parameter selection. They generated six candidate segmentation images using MS with different scale parameters, and defined the optimal parameter combination as the one resulting in an image which has maximal spectral seperability among seven predefined cover classes.

In the majority of cases, the above methods are used for segmenting spectral data. In the context of vegetation structure, the assumption is that it can be described by spectral information. While this is generally true, a much more detailed description of structure can be obtained by spatial data that is acquired by LiDAR or RADAR. Segmentation of LiDAR data has been seldom attempted before (although segmentation of three-dimensional data is a common procedure in other fields, especially medical imaging). Hyyppä *et al*. (2001) used a semi-automated segmentation method to delineate individual trees from LiDAR data in southern Finland. Mason *et al.* (2003), using a segmentation algorithm by Cobby *et al.* (2001), segmented LiDAR data to identify average height, shape and boundary structure of agricultural fields that serve as habitat for skylarks. Several land cover units (including forests of different age classes) were mapped by segmentation of LiDAR imagery of the Verdun area in France (Antonarakis *et al*. 2008). Similarly, Brennan and Webster (2006) conducted an object-based classification using range and intensity LiDAR data, and were able to successfully identify ten land cover classes in a coastal area in Nova Scotia. Mustonen *et al*. (2008) delineated forest stands in Finland by visual interpretation, and by applying MS to a colour aerial photo, a small footprint LiDAR, and a combination of both. The results were compared to field measurements of stand characteristics, and revealed that, in most cases, using MS with height solely yielded the best results.

While there are clear criteria for defining forest stands in the regions mentioned above, in Mediterranean landscapes this is much more complex, since they often consist of a fine-scale mosaic of woodlands, shrublands and herbaceous clearings, all with varying heights and densities. In most cases, structural-based management

units are mapped using manual interpretation of aerial imagery coupled with fieldwork. Since distinct boundaries between different structures of vegetation seldom exist in Mediterranean vegetation, manual delineation of structural-based units cannot be ubiquitous. We therefore suggest that delineation of vegetation structural units (which could later serve as the foundations of management units) should arise from the continuous spatial distribution of height and cover within each landscape. The height/cover continua could be divided into distinct units using automated image segmentation approaches. To the best of our knowledge, there are no studies that have attempted to delineate vegetation units using structural traits in such complex landscapes using automated segmentation methods.

The objective of this research is to develop a methodology for automated mapping of vegetation units, based on two structural characteristics of vegetation: height and cover. For achieving this purpose we combine both pixel-based and object-based classifications of LiDAR imagery and segmented LiDAR imagery, respectively, to yield coherent vegetation units which are amenable for planning and management.

2. Methods

2.1 *Study site*

The study was conducted at Ramat Hanadiv Nature Park, located at the southern tip of Mt Carmel, northern Israel (32° 30′ N, 34° 57′ E, figure 1). The area is a plateau with a mean elevation of 120 m above sea level (a.s.l.), descending steeply towards the coastal plain in the west via a series of rock cliffs, and descending gently towards the Hanadiv Valley in the south-east. The parent rock formations consist of limestone and dolomite, with a volcanic marly tuff layer below the upper limestone layer. The soil in the area is mainly Xerochreps, developed on hard limestone or dolomite (Kaplan 1989). The climate is eastern Mediterranean, with an average annual rainfall of 600 mm, occurring mostly between November and March. The vegetation is also mostly eastern Mediterranean scrubland and shrublands, dominated by dwarf shrubs (*Sarcopoterium spinosum*), low summer deciduous shrubs (*Calycotome villosa*), evergreen medium-sized shrubs (*Pistacia lentiscus*) and evergreen tall shrubs (*Phillyrea media*). Additionally, several scattered forest groves exist in the area, consisting primarily of conifer plantations (mainly *Pinus halepensis*, *Pinus brutia*, and *Cupressus sempervirens*). The park hosts a very rich flora of annuals and geophytes in open patches (Hadar *et al*. 1999, 2000). The landscape structure is a fine-grain mosaic of woody patches of different heights and sizes, herbaceous clearings, exposed rock and bare ground (Perevolotsky *et al*. 2002).

2.2 *LiDAR data*

A LiDAR point cloud was acquired by Ofek™ in 2005, with an Optech™ ALTM2050 LiDAR (Optech Inc., Toronto, ON, Canada) which operates at 50 000 Hz, and recorded the first return for each laser pulse. Flight altitude was 1500 m, and LiDAR strips were acquired with a 33° maximum scan angle and 30% side overlaps. Following geocorrection, the vertical accuracy of the LiDAR points was 0.15 m, and the planimetric accuracy was 0.75 m.

A digital elevation model (DEM, representing ground height) was generated by overlaying the LiDAR on a colour orthophoto (0.25 m pixel size), identifying LiDAR hit-points that were located on the ground, and interpolating the data from these points to create a 2 m grid. In order to derive the height of each point, the DEM

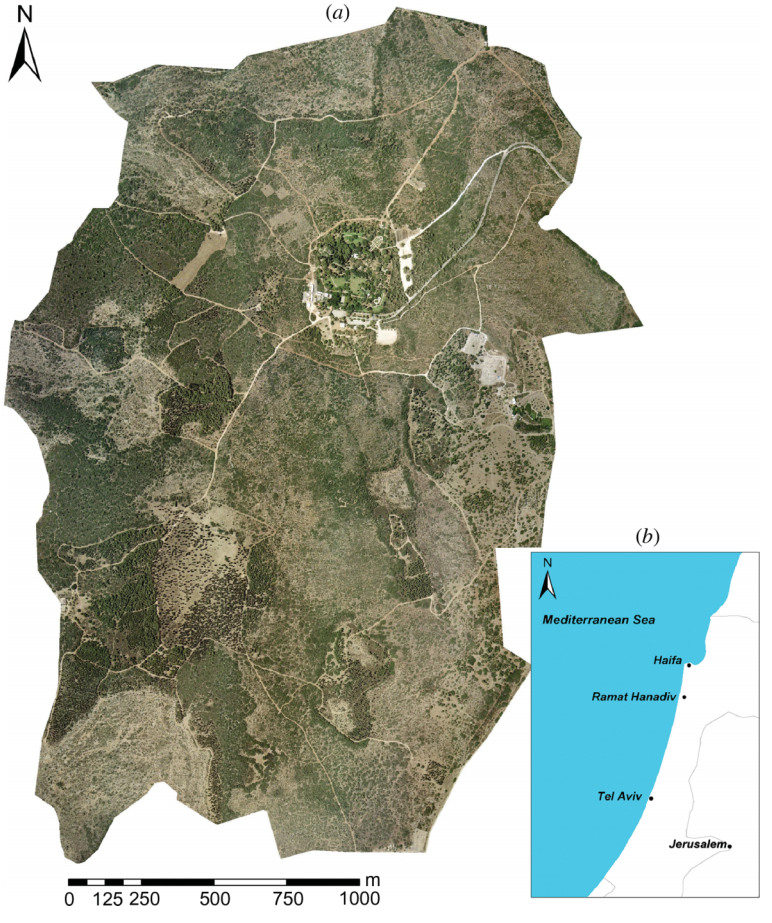

Figure 1. Aerial photograph of the study area, (*a*) Ramat Hanadiv Nature Park and (*b*) its location in Israel.

value underneath each point was subtracted from the point elevation. A digital terrain model (DTM, representing top height, either canopy or bare ground) of the landscape was derived by calculating the maximal height of points within a grid of 4 m sized pixels, which was superimposed on the data (figure 2(*a*)). A spatial resolution of 4 m was used since it roughly fits the average size of fully grown shrubs in the study area. The average number of LiDAR samples per 4 m pixel was 28.2.

A woody cover data layer that overlapped the DTM was created in the following manner. It was assumed that woody vegetation was taller than 0.2 m. The DTM was then reclassified into a binary image of two classes: woody vegetation and background (consisting of herbaceous vegetation, rocks and ground). In each pixel, the number of woody points was calculated, divided by the total number of points (woody + background), and the product multiplied by 100 to convert to percentage of woody cover (figure 2(*b*)).

2.3 *Automated segmentation of the DTM and cover layer*

MS (Baatz and Schäpe. 2000, Benz *et al*. 2004) was used, implemented in eCognition™ (Trimble, Sunnyvale, CA, USA) (Benz *et al.* 2004), to segment the DTM

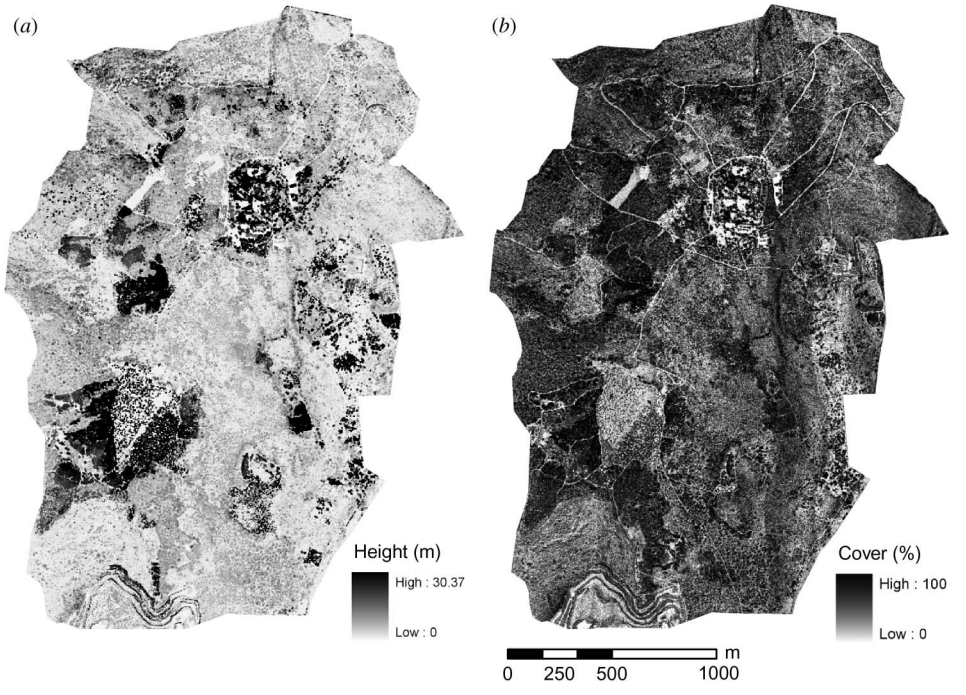

Figure 2. Map layers of the study area: (*a*) maximum height and (*b*) woody cover.

and woody cover layer into discrete polygons. MS operates in a bottom-up approach, using a region merging technique that starts with one-pixel objects, which are subsequently merged into larger image objects. Adjacent image objects are merged as long as the increase in object heterogeneity is lower than a certain threshold defined as:

$$f = w_{\text{colour}} \times \Delta h_{\text{colour}} + w_{\text{shape}} \times \Delta h_{\text{shape}}, \tag{1}$$

where f is the scale parameter, which represents the threshold to the increase in heterogeneity of image objects, w_{colour} and w_{shape} are user-assigned weights to the differences in spectral heterogeneity Δh_{colour} and shape heterogeneity Δh_{shape}, respectively. The difference in spectral heterogeneity is defined as:

$$\Delta h_{\text{colour}} = w_{\text{c}} \left(n_{\text{merge}} \times \sigma_{\text{c,merge}} - \left(n_{\text{obj\_1}} \times \sigma_{\text{c,obj\_1}} + n_{\text{obj\_2}} \times \sigma_{\text{c,obj\_2}} \right) \right), \tag{2}$$

where w_{c} is the weight of the input band c (here, height or cover), n_{merge} the number of pixels in the merged image object, $n_{\text{obj\_1}}$ and $n_{\text{obj\_2}}$ are the numbers of pixels in objects 1 and 2 (prior to the merge), respectively, and $\sigma_{\text{c,obj\_1}}$ the standard deviation of pixel values in an object of band c.

The difference in shape heterogeneity represents the change in object shape in terms of smoothness and compactness:

$$\Delta h_{\text{shape}} = w_{\text{compt}} \times \Delta h_{\text{compt}} + w_{\text{smooth}} \times \Delta h_{\text{smooth}}, \tag{3}$$

where the smoothness heterogeneity denotes the ratio between the border length l of an image object and the border length b of the bounding box of that image object:

$$\Delta h_{\text{smooth}} = n_{\text{merge}} \times \frac{l_{\text{merge}}}{b_{\text{merge}}} - \left(n_{\text{obj\_1}} \times \frac{l_{\text{obj\_1}}}{b_{\text{obj\_1}}} + n_{\text{obj\_2}} \times \frac{l_{\text{obj\_2}}}{b_{\text{obj\_2}}} \right). \quad (4)$$

The compactness heterogeneity denotes the ratio between the border length l of an image object and the square root of the number of pixels in that object:

$$\Delta h_{\text{compt}} = n_{\text{merge}} \times \frac{l_{\text{merge}}}{\sqrt{n_{\text{merge}}}} - \left(n_{\text{obj\_1}} \times \frac{l_{\text{obj\_1}}}{\sqrt{n_{\text{obj\_1}}}} + n_{\text{obj\_2}} \times \frac{l_{\text{obj\_2}}}{\sqrt{n_{\text{obj\_2}}}} \right). \quad (5)$$

The user of MS needs to specify six parameters, which are the scale parameter (f), weights of input layers (w_c), spectral heterogeneity (w_{colour}), shape heterogeneity (w_{shape}), smoothness (w_{smooth}) and compactness (w_{compt}).

The large number of possible parameter combinations, coupled with their abstract nature as far as the segmentation process is concerned, implies that it is not possible to predefine an entire set of parameters that will result in an optimal segmentation (Wang *et al.* 2004, Hay *et al.* 2005). Therefore, a set of segmentation results were generated rather than a single output. To limit the number of results, the colour, shape, smoothness and compactness parameters were set to constant values throughout the simulations, and only the weights of the input layers and the scale parameter changed. Colour/shape were set to 0.9/0.1 (i.e. most emphasis was put on the heterogeneity of height and cover values), and smoothness/compactness were set to 0.5/0.5, respectively.

Height data had a much lower variance than cover data, so had to be assigned larger weights in MS. The range of layer weights were therefore tested between 80% and 100% height (while cover weights completed the height weights to 100%). Testing a height layer weight of 100% implies that cover has no direct effect on the segmentation process. Yet, there was some degree of correlation between height and cover in the study area (i.e. higher pixels also had larger cover values) and thus cover affected the segmentation process indirectly even when its weight was set to 0. The scale parameter was tested between 10 (expected segment sizes are small, with good distinction between segments) and 50 (expected segments are large) in increments of five. This range was chosen following initial tests which revealed that scale parameter values smaller than 10 generated severe over-segmentation, while scale parameter values above 50 resulted in severe under-segmentation, with both results being inadequate for our mapping purposes.

The resulting image segments were classified into distinct height/cover categories using a classification scheme developed by the managers of the study area, based on a combination of the schemes presented by Naveh and Whittaker (1979) and by Tomaselli (1981). It comprised four height categories: 0–0.5 m (low), 0.5–2 m (medium), 2–5 m (tall), >5 m (very tall) and four cover categories: <25% (open), 25–50% (scattered), 50–75% (discontinuous) and >75% (dense). The segmented height/cover images were overlaid on the woody height and woody cover data layers. Each pixel was assigned to its corresponding class according to the values derived from the original data layers. Then, each segment was assigned to the class to which the majority of its pixels belonged. In the final step, adjacent segments that were assigned to the same class were merged into a single, larger segment.

2.4 *Map comparison*

Since there were many resulting segmentation maps, each corresponding to a candidate delineation of structural units, they were compared to reference units using an approach developed for accuracy assessment of segmentation algorithms (Lucieer and Stein 2002). The height and cover layers were combined into a red, green and blue (RGB) image that represents a continuous vegetation structure map (figure 3). A human interpreter then delineated 20 structural units in that map. Each unit had to be

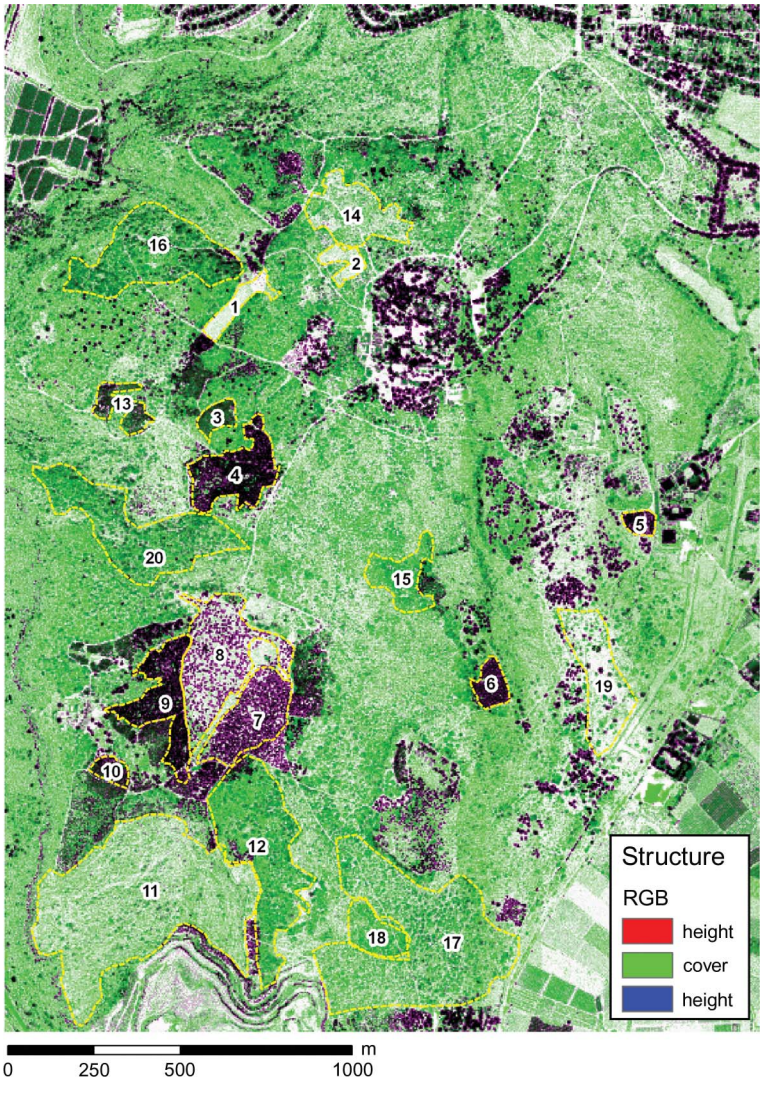

Figure 3. The continuous vegetation structure map and the reference units. Darker pixels represent tall and dense vegetation, brighter pixels represent low and sparse vegetation or open landscape/bare soil. Green pixels represent low and dense vegetation (greener is denser), while purple pixels represent tall and sparse vegetation (usually tall individual trees with no understorey vegetation). Reference units are numbered and outlined by dashed yellow lines.

clearly separated from its surrounding vegetation in terms of structure. The units consisted of pine stands, open fields, an open and low shrubland surrounded by conifers and several shrubland areas with varying vegetation height and woody cover.

The accuracy of each automated segmentation map relative to the reference units was assessed using the area-fit index (AFI; Lucieer and Stein 2002). AFI measures the degree of overlap between a reference unit and its largest overlapping segment object. There are three potential relations between the reference and segmentation objects: (1) perfect fit (100% overlap between the reference and a segment); (2) over-segmentation (there is more than one segment in a reference unit, less than 100% overlap); (3) under-segmentation (the reference unit is fully contained in a larger segment, more than 100% overlap). AFI calculates the relation between the areas of the reference object and its largest overlapping segmentation object in the following way:

$$\mathrm{AFI} = \frac{A_{\mathrm{reference}} - A_{\mathrm{segment}}}{A_{\mathrm{reference}}}, \tag{6}$$

where $A_{\mathrm{reference}}$ and A_{segment} are the areas of the reference and segmented objects, respectively. When AFI is 0, there is a perfect fit between the reference and segmented objects. Positive AFI represents over-segmentation and negative AFI represents under-segmentation. AFI was calculated for each one of the ten reference units, for the 45 segmentation maps. The area-weighted average AFI per map was used to determine the segmentation product that is most similar to the reference objects.

The selected segmentation map was compared to a map of botanical vegetation formations (Sagie *et al*. 2000), which has been used for management purposes in the study area, in order to assess the difference between our method and the common approach for mapping vegetation units in Israel. This map was generated by manual delineation of aerial photos coupled with field surveys. It consists of 18 classes of vegetation formations and other, human-made, cover types (table 1). Natural vegetation is described either by the dominant species or by the traditional Mediterranean classification (e.g. maquis, garrigue, etc.), in addition to its density (e.g. dense garrigue, open park woodland, sparse pine).

The comparison was carried out by categorical correspondence analysis in which the amount of overlap among different structural classes and vegetation formation classes was quantified. Our major aim in developing the structural mapping approach is not to correspond well to the botany-based approach, but rather to provide an alternative that does not rely on botanical definitions. In addition, though there was a five-year gap between the vegetation formations map and the LiDAR survey presented here, field measurements revealed that the vegetation in the study areas has changed very little during that period, thus it was assumed that the correspondence analysis was valid.

3. Results

3.1 *Height and cover in the study area*

The height of the vegetation in the study area was generally low, with an average maximum of 2.18 m for the entire landscape, which characterizes the predominant shrub species *Pistacia lentiscus* and *Phillyrea media* (figure 2(*a*)). The largest height value for a pixel was 30.36 m, and it was located in an area dominated by *Pinus*

Table 1. Vegetation formations in the classification scheme used for the manual mapping of Ramat Hanadiv, showing the proportion of each vegetation formation in the study area. Data is from Sagie *et al*. (2000).

Formation	Percentage of the study area (%)
Sparse pine	5.40
Dense pine	4.55
Pistacia shrubland	2.62
Vineyard	3.80
Sparse cypress	4.24
Dense cypress	2.92
Garrigue	0.15
Sparse garrigue	1.19
Dense garrigue	0.15
Maquis	15.81
Sparse maquis	41.76
Dense maquis	8.00
Park woodland	1.33
Open park woodland	2.67
Sparse herbaceous	0.01
Dense herbaceous	1.98
Riparian vegetation	0.04
Other/non-vegetated	0.09

halapensis (Aleppo pine) trees. The average cover of the pixels was 54.45% (figure 2(*b*)). The distribution of cover in the study area had two distinctive peaks at zero cover (open areas) and 100% cover, but the majority of pixels exhibited intermediate cover. Thus, the majority of the study area consisted of low and relatively dense vegetation. The continuous vegetation structure map that was used for the manual interpretation step (figure 3) portrays clearly the large structural heterogeneity of the vegetation in the study area. The continuum of height/cover combinations ranged from low-open pixels, representing herbaceous patches (as well as roads and other artificial surfaces) to tall-dense pixels, usually corresponding to pine and cypress plantations.

3.2 *Segmentation results*

The 45 parameter combinations (9 scale parameters × 5 height/cover combinations) resulted in a wide array of segmentation maps, characterized by varying numbers of segments and segment sizes. As expected, low values of the scale parameter yielded many small segments, while high values yielded larger segments, but also larger variability in segment sizes. The number of segments decreased (from 1358 to 32) and their average size increased (from 3394 to 144 160 m^2) with increasing scale parameter. The scale parameter had a non-linear effect on the number of segments. For scale parameter values between 10 and 25, there was a sharp drop in the number of segments, while for values larger than 25, there was relatively little change.

The relative weight of height and cover affected segmentation results as well. Increasing the weight of woody cover resulted in an increase in the number of segments and a decrease in their sizes. For a given scale parameter value, a 20% change in the weight of the cover layer (from 0% to 20%) decreased the mean segment size by nearly half and doubled the number of segments.

3.3 *Segmentation accuracy*

In general, lower scale parameters delineated the reference units more accurately (figure 4). The area-weighted mean AFI for scale parameter 20% and 85% height was −0.003, two to three orders of magnitude better than most of the AFIs. It was followed by the scale parameter of 15% with 80% height (AFI = 0.006), with all other AFIs larger than 0.1. However, when calculating AFI for single reference units (rather than the average AFI), there was a large variation in the accuracy of the segmentation maps based on different parameter combinations. Three of the reference units were seldom delineated in an acceptable degree of accuracy (units 2, 3 and 18 in figure 3). These were also three of the six smallest reference units, with areas smaller than 1 ha. However, unit 5, which had an area of 0.58 ha, was delineated accurately in 40 of the 45 parameter combinations, thus area itself was not the sole determinant of segmentation accuracy.

The most accurate segmentation (scale parameter 20% and 85% height) was characterized in many cases by highly convolved edges and small segments. It contained 240 segments, with an average area of 1.92 ha. The convolved edges were mostly located in areas where there was a gradual change between shrubland structural classes. In these cases, the convolving edges followed the outline of individual shrubs that stood out relative to their surroundings.

According to the most accurate segmentation result, the major structural class in the study area was medium/scattered vegetation (0.5–2 m tall, 0.25–50% cover), which in this area corresponds to shrubland formations dominated by the evergreen shrubs *Phillyrea media* and *Pistacia lentiscus* (table 2, figure 5(*a*)). Medium height

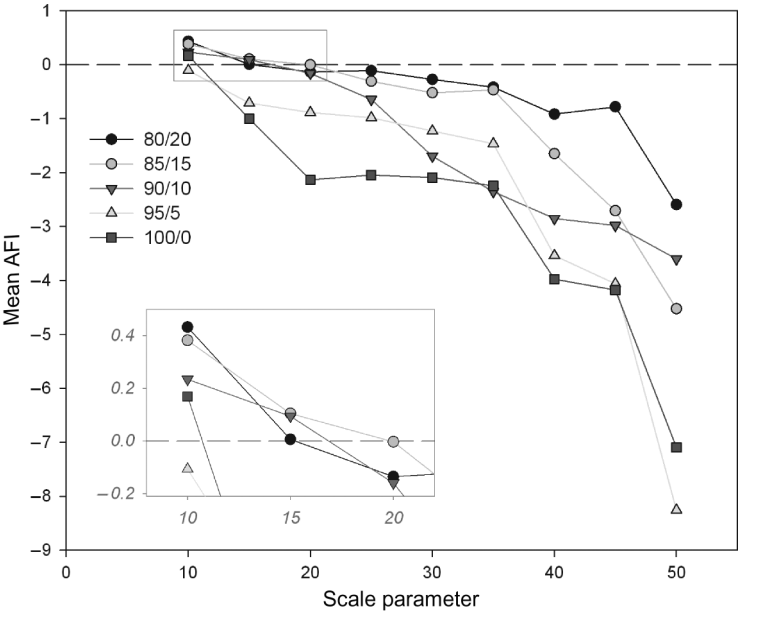

Figure 4. Effects of changing scale parameter on area-weighted mean AFI for 20 reference units. Each curve corresponds to different height/cover weights. Near-zero AFI values represent good agreement between reference and segmented objects. Inset: mean AFI values for scale parameters 10–20.

Table 2. The proportion of each structural class in the study area based on the most accurate segmentation map. The following classes do not exist in the resulting segments: low/discontinuous, low/dense and tall/open.

Class code	Class name	Percentage of area (%)
11	Low/open	7.58
12	Low/scattered	2.10
21	Medium/open	0.84
22	Medium/scattered	35.16
23	Medium/discontinuous	23.73
24	Medium/dense	6.88
32	Tall/scattered	0.02
33	Tall/discontinuous	2.05
34	Tall/dense	11.32
41	Very tall/open	0.40
42	Very tall/scattered	0.07
43	Very tall/discontinuous	2.37
44	Very tall/dense	7.48

structural classes covered 66.61% of the study area, while very tall structural classes (height > 5 m), which represent *Pinus halepensis*, *P. brutia* and *Cupressus sempervirens* plantations, covered 10.32% of the study area. There were no segments representing the low-discontinuous and low-dense classes (<0.5 m, 50–100% cover), indicating that lower vegetation types seldom appear in dense patches in this segmentation result. Similarly, there were no tall/open segments, meaning that taller vegetation types are seldom scattered in open areas in the study area. In addition, tall and very tall vegetation classes (2.5 m and above) tended to appear in dense cover areas (over 75% cover).

3.4 *Comparison with a vegetation formations map*

The area correspondence analysis between the vegetation formations map (Sagie *et al*. 2000) and the new structure map revealed that in all cases, vegetation formations were described by several structural classes (table 3, figure 5). The most dominant formation in the study area, sparse maquis (41.3% of the study area) consisted of 57.37% medium/scattered vegetation and 28.39% medium/discontinuous vegetation (with eight other structural classes having lower overlap). Thus, the broadly defined maquis formation consisted of several structural classes which represent a gradient of woody vegetation densities, and to a lesser extent heights. Similarly, the second most common formation in the study area, maquis (15.38%), consisted of a mixture of several structural classes, such as medium/discontinuous (29.91%), medium/scattered (23.74%), tall/dense (20.23%) and medium/dense (16.74%). Overall, the medium/scattered structural class was a dominant component in seven vegetation formations (sparse garrigue, garrigue, *Pistacia* shrubland, sparse maquis, maquis, open park woodland and park woodland), with areal correspondence values between 23.74% and 57.69%. However, all of these formations were also described by other structural classes, which highlights the significant structural variability within each formation.

The tall formations, including pine and cypress plantations, corresponded mostly with the very tall/dense and very tall/discontinuous structural classes, though in both cases they were represented by lower structural classess as well. This was especially

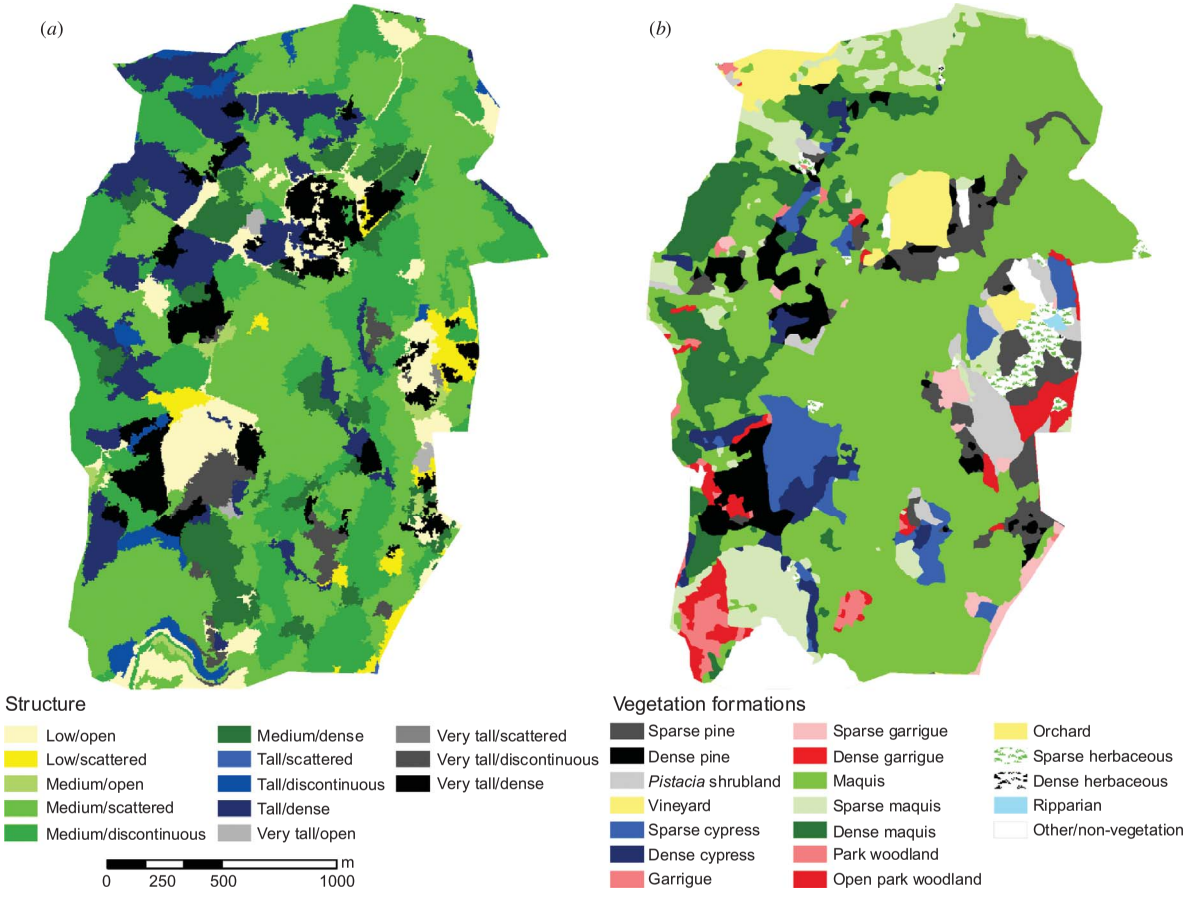

Figure 5. (*a*) The best vegetation structure map and (*b*) the vegetation formations map (Sagie *et al*. 2000) of the study area. In the structure map, colours vary according to height (yellow, green, blue and grey, for low, medium, tall and very tall vegetation, respectively), and cover (from bright to dark for open to dense vegetation, respectively).

Table 3. Correspondence among structural classes (columns) and vegetation formations (rows). Numbers represent the percentage of each structural class within each vegetation formation (rows sum to 100%), and high values appear in bold. Abbreviations: 'scat' is scattered, 'med' is medium, 'disc' is discontinuous. The man-made 'vineyard' and 'other' formation categories were omitted from the table.

Structure Formation	Low/ open (%)	Low/ scat (%)	Med/ open (%)	Med/ scat (%)	Med/ disc (%)	Med/ dense (%)	Tall/ scat (%)	Tall/ disc (%)	Tall/ dense (%)	Very tall/open (%)	Very tall/scat (%)	Very tall/disc (%)	Very tall/dense (%)
Sparse herbaceous	**40.57**	23.35	0.00	18.40	8.54	2.34	0.00	0.19	0.87	0.00	0.51	1.40	3.83
Dense herbaceous	0.00	0.00	0.00	16.67	**81.58**	0.00	0.00	0.00	1.75	0.00	0.00	0.00	0.00
Sparse garrigue	9.66	13.94	0.00	**50.33**	17.07	5.45	1.28	0.00	2.24	0.00	0.00	0.03	0.00
Garrigue	1.33	0.44	0.00	**52.00**	26.22	4.67	0.00	6.22	4.00	0.00	0.00	0.00	5.11
Dense garrigue	0.00	0.00	0.00	7.08	19.41	0.00	0.00	**55.71**	9.59	0.00	0.00	0.00	8.22
Pistacia shrubland	2.39	1.69	3.57	**44.99**	**43.12**	1.36	0.00	0.00	1.08	0.15	0.00	1.39	0.27
Sparse maquis	4.22	1.24	0.36	**57.37**	28.39	5.16	0.00	0.43	1.98	0.00	0.00	0.24	0.62
Maquis	1.84	0.78	0.23	**23.74**	**29.91**	16.74	0.00	3.36	**20.23**	0.12	0.00	0.27	2.78
Dense maquis	0.08	0.04	0.30	4.06	**30.32**	11.69	0.00	3.10	**49.20**	0.01	0.00	0.00	1.20
Open park woodland	10.88	1.51	7.29	**48.98**	21.36	1.01	0.00	0.38	3.58	1.86	0.08	0.27	2.81
Park woodland	3.65	0.00	0.03	**57.69**	9.70	16.51	0.00	2.30	7.19	2.94	0.00	0.00	0.00
Riparian	0.00	28.06	0.00	3.96	26.62	0.00	0.00	0.00	0.00	0.00	0.00	0.00	**41.37**
Sparse cypress	**38.58**	7.15	0.00	16.11	5.85	0.33	0.00	0.01	1.66	1.83	0.00	**26.42**	2.05
Dense cypress	3.73	0.00	0.00	9.50	6.81	2.90	0.00	5.10	18.53	0.00	0.00	**26.60**	**26.83**
Sparse pine	12.10	6.66	1.87	12.08	13.95	11.13	0.00	0.00	5.22	3.69	1.10	0.78	**31.42**
Dense pine	2.66	0.03	0.37	3.22	7.75	1.93	0.00	1.79	20.32	0.21	0.00	0.68	**61.03**
Orchard	8.61	0.30	0.00	7.72	18.48	0.01	0.00	6.78	**29.98**	0.00	0.00	0.00	**28.12**

evident for the sparse cypress formation, which occurred 38.58% of the time in the low/open structural class. This was caused by the majority rule that was the basis for the classification of segments. This rule forced areas of low density tree populations to be merged with their background, in this case herbaceous vegetation (see reference unit 8).

Overall, there was a considerable difference between the spatial patterns depicted by both maps, suggesting that in many cases vegetation formations do not represent the structural variation of vegetation in a cohesive way. This was especially true for the widely used class of maquis (Mediterranean shrubland/woodland) which, in practice, may consist of many structural classes based on density variations.

4. Discussion

Mapping structural vegetation units is a complicated task, since vegetation structure often changes in a gradual way across landscapes, without clear boundaries between distinctive structural units. This is especially true for Mediterranean systems, since these landscapes are characterized by highly heterogeneous and spatially complex vegetation formations. This heterogeneity occurs at many spatial scales simultaneously, further complicating attempts of mapping the vegetation in a manner that is both geographically robust and spatially realistic. The common approach to map Mediterranean vegetation incorporates subjective human decisions, either in the mapping technique (manual delineation of polygonal semi-homogeneous units) or the concept (using the dominant species as surrogates of vegetation formation), or both. Owing to the heterogeneity at fine scales, and the often gradual transitions between units, it is not possible to manually map vegetation in a robust manner over large areas. A map of vegetative formations (shrubland, garrigue etc.) is not sufficient in describing vegetation structure since Mediterranean vegetation is very dynamic and low shrubs quite rapidly become tall and even develop into trees, depending on the disturbance regime and microhabitat conditions. In addition, the dominant species vary among different subregions of the Mediterranean, and the existing naming conventions for vegetation formations are general and vary between countries. Consequently, much detail is lost in the attempts to map the vegetation using existing thematic classes such as vegetation formations. Furthermore, many existing vegetation maps have either thematic classes that are too general or consist of classes that are locally specific, and therefore cannot be directly compared to maps from other regions. Vegetation maps that would be thematically consistent over large areas would facilitate comparisons between different subregions.

In this study, we mapped Mediterranean vegetation using a different approach. We accounted only for the structural characteristics of vegetation that can be measured in a robust manner by remotely sensed data, in this case LiDAR. We then used an automated image segmentation algorithm, MS (Baatz and Schäpe 2000), to delineate distinct units from height and cover data obtained from LiDAR measurements. These units may serve as structure-based management units, which are emerging as an alternative to the commonly used botanically based units. In essence, this is an object-based approach to mapping vegetation, and it follows the general framework that has been successfully applied before to map riparian areas (Johansen *et al.* 2007), coastal mangrove forests (Wang *et al*. 2004), boreal forests (Chubey *et al.* 2006) and temperate forests (Antonarakis *et al*. 2008) at large spatial scales, and individual tree crowns at small spatial scales (Lucas *et al.* 2008). However, an inherent drawback of existing

segmentation algorithms is the difficulty to predict the effect of parameter selection on the outcome of the process (Hay *et al*. 2005). We therefore took an exploratory approach, in which many parameter combinations were used to create alternative segmented maps (Lamonaca *et al*. 2008). Wang *et al.* (2004) used the spectral properties of segments generated by a suite of segmentation parameters to identify the optimal parameter set (that produced maximal spectral seperability among segments). In contrast, we used a geometrical approach, where we selected the most accurate map using the AFI metric of Lucieer and Stein (2002). AFI quantifies the similarity among segmented objects and reference units, which in our study were delineated by a human interpreter. A single segmentation map stood out as the best alternative according to the accuracy metric we used (AFI).

The accuracy of the resulting map is affected by the choice of reference units. Any attempt to segment vegetation structure maps involves the transformation of continuous spatial data into discrete units, and, as such, varies with purpose and context. Thus, the choice of reference units should be based on *a priori* assumptions about the desired properties of the resulting maps (i.e. size and shape of structural units) in regard to actual management considerations. In addition, in many cases it is not possible to manually delineate ubiquitous boundaries between shrubland areas (as there are gradual transitions rather than clear edges between them). In those cases, the choice of reference unit is somewhat arbitrary, based on the subjective decision of the human interpreter regarding the 'correct' border between adjacent structural units. This problem is an inherent property of natural vegetation everywhere, but in Mediterranean regions it is especially pronounced owing to the spatial complexity of the vegetation at varying spatial scales.

While the method performed well for the majority of structural classes, we found that mixtures of low-density tall vegetation (especially pine and cypress trees) with lower vegetation types (especially herbaceous areas) could have resulted in misclassification. The sparse cypress plantation, which was delineated by reference unit 8, was classified as low/herbaceous structure. The correspondence analysis with the vegetation formations map revealed other areas where sparse tall vegetation was classified as low vegetation. This is a direct result of the classification algorthim, in which we determined the structural class based on the majority of the individual pixel classes within each segment, rather than using the average height/cover per segment. Thus, areas of low cover of tall vegetation were obscured by their high-cover low-height background, resulting in a low height class for the entire segment. We used the majority rule since using the alternative, segment-based average, would have reduced the detectability of open herbaceous segments, which are important for conservation in Mediterranean systems. The existence of few taller pixels might have elevated the average height to more than 0.5 m, defining the segment as a medium height unit, which often corresponds with shrubland vegetation.

5. Conclusion

Regardless of the limitations of the approach taken here, a comparison of the structural map and a commonly used vegetation formations map revealed that there is a wealth of new information that arises from using structure as an alternative descriptor of vegetation formations. One of the most common vegetation formations in the Mediterranean region, the maquis, may be characterized by various structural classes,

which are often overlooked when human interpreters attempt to construct vegetation maps. Vegetation in Mediterranean regions is constantly altered and manipulated by varying disturbances (Naveh and Kutiel 1986). These disturbances affect the structure of woody vegetation but have less impact on woody species composition owing to the inherent regeneration capability of many species (Arianoutsou 1998). Moreover, during the course of succession, vegetation constantly shifts between structures, usually from low and open vegetation to tall and dense vegetation, with disturbances switching the direction of these shifts through time and space (Westoby *et al*. 1989). It is therefore desirable that the mapping methodology we use to document these areas would enable us to follow the rapidly occurring structural changes. A structural mapping approach, such as presented here, is a promising methodology in this respect.

Acknowledgement
The research was funded by the Israel Science Foundation (grant 625/05).

References

Antonarakis, A.S., Richards, K.S. and Brasington, J., 2008, Object-based land cover classification using airborne LiDAR. *Remote Sensing of Environment*, **112**, pp. 2988–2998.

Arianoutsou, M., 1998, Aspects of demography in post-fire Mediterranean plant communities of Greece. In *Ecological Studies. Vol. 136, Landscape degradation and biodiversity in Mediterranean-Type Ecosystems*, P. Rundel (Ed.), pp. 273–295 (Berlin: Springer-Verlag).

Baatz, M. and Schäpe, A., 2000, Multiresolution segmentation – an optimization approach for high quality multi-scale image segmentation. In *Angewandte Geographische Informations-Verarbeitung XII*, J. Strobl, T. Blaschke and G. Griesebner (Eds.), pp. 12–23 (Karlsruhe: Wichmann Verlag).

Bar Massada, A., Gabay, O., Perevolotsky, A. and Carmel, Y., 2008, Quantifying the effect of grazing and shrub-clearing on small scale spatial pattern of vegetation. *Landscape Ecology*, **23**, pp. 327–339.

Benz, U.C., Hofmann, P., Willhauck, G., Lingenfelder, I. and Heynen, M., 2004, Multiresolution, object-oriented fuzzy analysis of remote sensing data for GIS-ready information. *ISPRS Journal of Photogrammetry and Remote Sensing*, **58**, pp. 239–258.

Bergen, K.M., Gilboy, A.M. and Brown, D.G., 2007, Multidimensional vegetation structure in modeling avian habitat. *Ecological Informatics*, **2**, pp. 9–22.

Brennan, R. and Webster, T.L., 2006, Object-oriented land cover classification of LiDAR-derived surfaces. *Canadian Journal of Remote Sensing*, **32**, pp. 162–172.

Bunting, P. and Lucas, R., 2006. The delineation of tree crowns in Australian mixed species forests using hyperspectral compact airborne spectrographic imager (CASI) data. *Remote Sensing of Environment*, **101**, pp. 230–248.

Chubey, M.S., Franklin, S.E. and Wulder, M.A., 2006. Object-based analysis of Ikonos-2 imagery for extraction of forest inventory parameters. *Photogrammetric Engineering and Remote Sensing*, **72**, pp. 383–394.

Cobby, D.M., Mason, D.C. and Davenport, I.J., 2001, Image processing of airborne scanning laser altimetry for improved river flood modelling. *Journal of Photogrammetry and Remote Sensing*, **56**, pp. 121–138.

De Jong, S.M., Hornstra, T. and Maas, H.G., 2001, An integrated spatial and spectral approach to the classification of Mediterranean land cover types: the SSC method. *Journal of Applied Earth Observation and Geoinformation*, **3**, pp. 176–183.

Di Castri, F., 1981, Mediterranean-type shrublands of the world. In *Mediterranean-type Shrublands*, F. Di Castri, D.W. Goodall and R.L. Specht (Eds.), pp. 1–52 (Amsterdam: Elsevier).

Dufour Dror, J.M., 2002, A quantitative classification of Mediterranean mosaic-like landscapes. *Journal of Mediterranean Ecology*, **3**, pp. 3–12.

Goodwin, N.R., Coops, N.C. and Culvenor, D.S., 2006, Assessment of forest structure with airborne LiDAR and the effects of platform altitude. *Remote Sensing of Environment*, **103**, pp. 140–152.

Hadar, L., Noy-Meir, I. and Perevolotsky, A., 1999, The effect of shrub clearing and grazing on the composition of a Mediterranean plant community: functional groups versus species. *Journal of Vegetation Science*, **10**, pp. 673–682.

Hadar, L., Noy-Meir, I. and Perevolotsky, A., 2000, Scale-dependent effects of fuel break management on herbaceous community diversity in a Mediterranean garrigue. *Journal of Mediterranean Ecology*, **1**, pp. 237–248.

Hay, G.J., Castilla, G., Wulder, M.A. and Ruiz, J.R., 2005, An automated object-based approach for the multiscale image segmentation of forest scenes. *International Journal of Applied Earth Observation and Geoinformation*, **7**, pp. 339–359.

Hinsley, S.A., Hill, R.A., Gaveau, D.L.A. and Bellamy, P.E., 2002, Quantifying woodland structure and habitat quality for birds using airborne laser scanning. *Functional Ecology*, **16**, pp. 851–857.

Hyyppä, J., Kelle, O., Lehikoinen, M. and Inkinen, M., 2001, A segmentation-based method to retrieve stem volume estimates from 3-D tree height models produced by laser scanners. *IEEE Transactions on Geoscience and Remote Sensing*, **39**, pp. 969–975.

Johansen, K., Coops, N.C., Gergel, S.E. and Stange, Y., 2007, Application of high spatial resolution imagery for riparian and forest ecosystem classification. *Remote Sensing of Environment*, **110**, pp. 29–44.

Kaplan, Y., 1989, *The Soils of Ramat Hanadiv* (Tel Aviv: Society of Nature Protection) [In Hebrew].

Kuchler, A.W., 1988, A physiognomic and structural analysis of vegetation. In *Vegetation mapping*, A.W. Kuchler and I.S. Zonneveld (Eds.), pp. 37–43 (Dordrecht: Kluwer Academic Publishers).

Lamonaca, A., Corona, P. and Barbati, A., 2008, Exploring forest structural complexity by multi-scale segmentation of VHR imagery. *Remote Sensing of Environment*, **112**, pp. 2839–2849.

Lavorel, S., 1999, Ecological diversity and resilience of Mediterranean vegetation to disturbance. *Diversity and Distributions*, **5**, pp. 3–13.

Le Houerou, H.N., 1981, Impact of man and his animals on Mediterranean vegetation. In *Mediterranean type shrublands*, F. Di Castri, D.W. Goodall and R.L. Specht (Eds.), pp. 479–521 (Amsterdam: Elsevier).

Lobo, A., 1997, Image segmentation and discriminant analysis for the identification of land cover units in ecology. *IEEE Transactions on Geoscience and Remote Sensing*, 35, pp. 1136–1145.

Lucas, R.M., Lee, A.C. and Bunting, P.J., 2008, Retrieving forest biomass through integration of CASI and LiDAR data. *International Journal of Remote Sensing*, **29**, pp. 1553–1577.

Lucieer, A. and Stein, A., 2002, Existential uncertainty of spatial objects segmented from satellite sensor imagery. *IEEE Transactions on Geoscience and Remote Sensing*, **40**, pp. 2518–2521.

Lucieer, A. and Stein, A., 2005. Texture-based landform segmentation of LiDAR imagery. *International Journal of Applied Earth Observation and Geoinformation*, **6**, pp. 261–270.

Mason, D.C., Anderson, G.Q.A., Bradbury, R.B., Cobby, D.M., Davenport, I.J., Vandepoll, M. and Wilson, J.D., 2003, Measurement of habitat predictor variables for organism – habitat models using remote sensing and image segmentation. *International Journal of Remote Sensing*, **24**, pp. 2515–2532.

Mustonen, J., Packalén, P. and Kangas, A., 2008, Automatic segmentation of forest stands using a canopy height model and aerial photography. *Scandinavian Journal of Forest Research*, **23**, pp. 534–545.

Naveh, Z., 1975, The evolutionary significance of fire in the Mediterranean region. *Plant Ecology*, **29**, pp. 199–208.

Naveh, Z. and Dan, J., 1973, The human degradation of Mediterranean landscapes in Israel. In *Mediterranean-type ecosystems (origin and structure)*, F. Di Castri and H.A. Mooney (Eds.), pp. 373–390 (Berlin: Springer-Verlag).

Naveh, Z. and Kutiel, P., 1986, Changes in the Mediterranean vegetation of Israel in response to human habitation and land use. In *The Earth in Transition, Patterns and Processes of Biotic Impoverishment*, G.M. Woodwell (Ed.), pp. 259–296 (Cambridge: Cambridge University Press).

Naveh, Z. and Whittaker, R.H., 1979, Structural and floristic diversity of shrublands and woodlands in northern Israel and other Mediterranean areas. *Vegetatio*, **41**, pp. 171–190.

Noy-Meir, I., Gutman, M. and Kaplan, Y., 1989, Responses of Mediterranean grassland plants to grazing and protection. *Journal of Ecology*, **77**, pp. 290–310.

Pausas, J.G., 1999, Mediterranean vegetation dynamics: modelling problems and functional types. *Plant Ecology*, **140**, pp. 27–39.

Perevolotsky, A., Ettinger, E., Schwartz-Tzachor, R. and Yonatan, R., 2002, Management of fuel brakes in the Israeli Mediterranean ecosystems: the case of Ramat-Hanadiv Park. *Journal of Mediterranean Ecology*, **3**, pp. 13–22.

Radoux, J. and Defourny, P., 2007, A quantitative assessment of boundaries in automated forest stand delineation using very high resolution imagery. *Remote Sensing of Environment*, **110**, pp. 468–475.

Sagie, Y., Lahav, H. and Levin, N., 2000, *Defining the Desired Landscape as a Foundation for Planning and Management of the Open Area in Ramat Hanadiv* (Tel Aviv: Society for the Protection of Nature in Israel).

Samet, H., 1990, *The Design and Analysis of Spatial Data Structures* (Reading, MA: Addison-Wesley).

Shoshany, M., 2000, Satellite remote sensing of natural Mediterranean vegetation: a review within an ecological context. *Progress in Physical Geography*, **24**, pp. 153–178.

Straatsma, M.W. and Middelkoop, H., 2006, Airborne laser scanning as a tool for lowland floodplain vegetation monitoring. *Hydrobiologia*, **565**, pp. 87–103.

Tomaselli, R., 1981, Main physiognomic types and geographic distribution of shrub systems related to Mediterranean climates. In *Mediterranean-type shrublands*, F. Di Castri, D.W. Goodall and R.L. Specht (Eds.), pp. 95–106 (Amsterdam: Elsevier).

Wang, L., Sousa, W.P. and Gong, P., 2004, Integration of object-based and pixel-based classification for mapping mangroves with IKONOS imagery. *International Journal of Remote Sensing*, **25**, pp. 5655–5668.

Westoby, M., Walker, B. and Noy-Meir, I., 1989, Opportunistic management for rangelands not at equilibrium. *Journal of Range Management*, **42**, pp. 266–274.